Hydrogen mediated ferromagnetism in ZnO single crystals

M. Khalid, P. Esquinazi

Division of Superconductivity and Magnetism, University of Leipzig, D-04103 Leipzig, Germany

D. Spemann

Division of Nuclear Solid State Physics, University of Leipzig, D-04103 Leipzig, Germany

W. Anwand, G. Brauer

Institut für Strahlenphysik, Forschungszentrum Dresden-Rossendorf, PO Box 510119, D-01314 Dresden, Germany

Abstract. We investigated the magnetic properties of hydrogen plasma treated ZnO single crystals by SQUID magnetometry. In agreement with the expected hydrogen penetration depth we found ferromagnetic behavior located at the first 20 nm of the H-treated surface of ZnO with magnetization at saturation up to 6 emu/g at 300 K and Curie temperature $T_c \gtrsim 400$ K. In the ferromagnetic samples a hydrogen concentration of a few atomic percent in the first 20 nm surface layer was determined by nuclear reaction analysis. The saturation magnetization of H-treated ZnO increases with the concentration of hydrogen.

PACS numbers: 75.70.-i, 75.20.Ck, 75.30.Hx, 75.50.Pp

Submitted to: *New J. Phys.*

After a large number of studies and different kinds of efforts, experimental and theoretical work of the last years indicate that defect-induced magnetism remains the key to trigger ferromagnetism in ZnO (as well as in other non-magnetic oxides) with Curie temperature above 300 K. Not the doping with magnetic elements appears to be a successful and reproducible method to trigger magnetic order in this oxide but the introduction of a certain defect density of the order of a few percent, like O- [1] or Zn-vacancies [2] with or without doping of non-magnetic ions like C [3], N [4], Li[5] or Cu [6, 7]. In general, however, the achieved magnetization values are still too low, indicating that the magnetic order is very probably not homogeneously distributed in the whole sample, a necessary condition for application of this phenomenon in ZnO-based devices.

What about the influence of hydrogen in the magnetism of ZnO? It is known that the presence of hydrogen is unavoidable in all systems and in general it remains rather difficult to measure it with high enough accuracy. Hydrogen related magnetic order was recently found in graphite surfaces by x-ray magnetic circular dichroism [8] indicating that this element can play a role in the magnetism of nominally non magnetic materials. The role of hydrogen in ZnO can be diverse. It can act either as donor (H^+) or acceptor (H^-) and can even modify the host structure. In bulk ZnO hydrogen acts as a shallow donor and is a source of the unintentional n-type conductivity [9]. Room temperature ferromagnetism due to atomic hydrogen adsorption on different terminated surfaces of ZnO [10, 11, 12] or in the bulk of Co-doped ZnO [13] has been studied theoretically. In one of these studies it was shown that atomic hydrogen adsorbed on the Zn place on the ZnO(0001) surface forms a strong H-Zn bonds leading to a metallic surface with a net magnetic moment [12]. All these theoretical studies indicate that it is important to check whether hydrogen implantation can trigger ferromagnetism in ZnO. In this work we investigate the magnetic properties of ZnO single crystals treated by remote hydrogen plasma and demonstrate that a remarkable ferromagnetic signal with a large magnetization is located in a few nm of the H-treated surface of the ZnO single crystals. Our finding opens up a simple and reproducible possibility to trigger magnetic order in broad or localized regions of ZnO bulk, thin films or microstructures without the need of introducing other elements or vacancies.

Hydrothermally grown ZnO single crystals were used for H-plasma treatment. Two of them were with one-side polished (O-terminated) of dimensions $\sim (10 \times 10 \times 0.5)$ mm^3 (MaTeck GmbH, Jülich). One of them was treated with H-plasma while the other one was kept as reference. Both single crystals were cut before treatment to directly mount them in a straw for the magnetic measurements done with a Superconducting Quantum Interferometer Device (SQUID). Four other crystals were two sides polished with similar termination but of dimensions $\sim (6 \times 6 \times 0.5)$ mm^3 (CrysTec GmbH, Berlin). Hydrogen doping in ZnO can be achieved by, e.g. adsorption of hydrogen on the ZnO surface, H-implantation or remote hydrogen plasma doping [14, 15, 16]. We used the last method to implant hydrogen into ZnO.

There are several parameters that may influence the strength of the magnetic order triggered through H-plasma treatment. Namely, the sample temperature, the H^+-ion

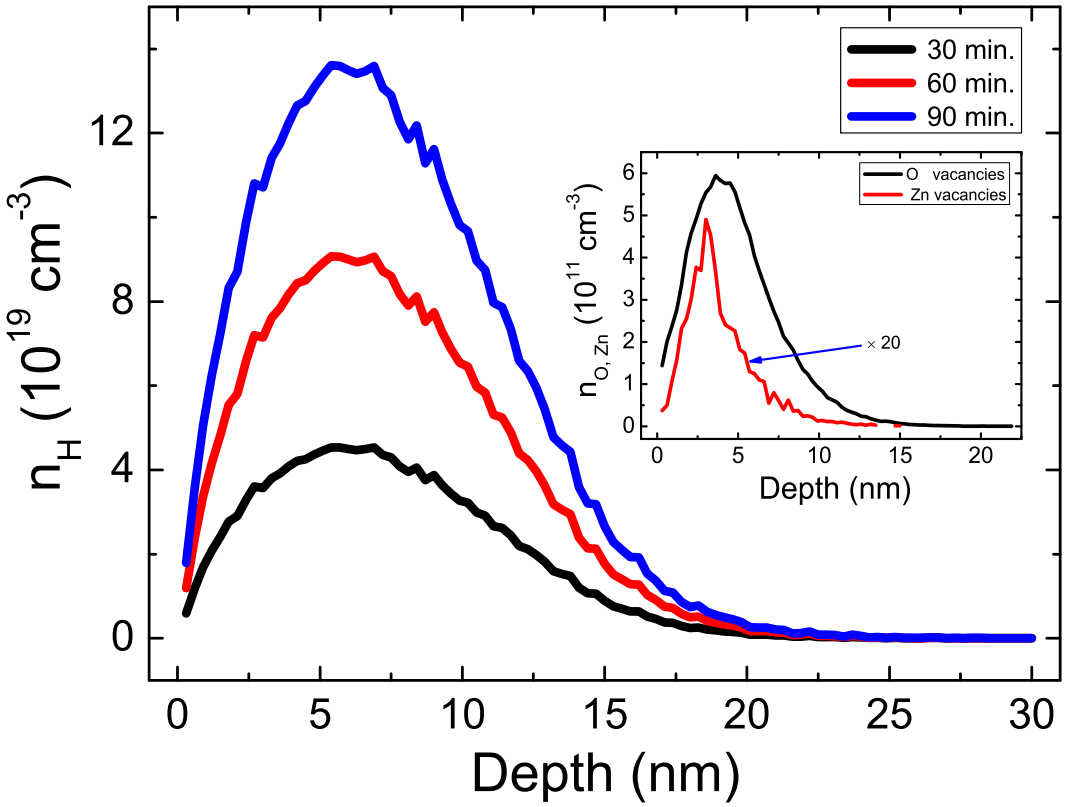

Figure 1. Hydrogen concentration vs penetration depth of H^+-ions in ZnO single crystals at different total implanted time, estimated by SRIM. The simulation results show that most of the H^+-ions are implanted within the first 20 nm from the surface. The inset shows the oxygen and zinc vacancies concentration produced in ZnO single crystals during 90 minutes H-implantation at the used energy conditions.

energy and current and the total implanted charge. In this work we demonstrate how the substrate temperature and the total implanted charge influence the magnetic ordering in ZnO crystals. The substrate temperature was varied from room temperature to 400 °C whereas the total implanted charge was controlled by varying the treatment time ranging from 30 to 90 min. The ZnO surface was placed ∼100 nm downstream from the plasma with a bias voltage of ∼-330 V (parallel-plate system of voltage difference of 10^3 V). The bias current was fixed at ∼ 50 μA (sample plus sample holder) while the current into the sample only was nA. The exposition to remote hydrogen dc plasma ranges from 30 to 90 min. During the loading the gas pressure was ∼1 mbar.

The hydrogen content before and after H-treatment was determined by standard Nuclear Reaction Analysis (NRA) [17] using 6.64 MeV ^{15}N ions with a depth resolution of ∼5 nm and a H detection limit of ∼200 ppm. The H-concentration vs. depth was obtained using SRIM (The Stopping and Range of Ions in Matter) simulation [18], see Fig. 1. The average hydrogen atomic concentration of bound hydrogen measured by NRA within the top 100 nm surface region of the ZnO crystals before and after 60 min treatment was (0.14±0.03) and (0.64±0.07) at.%, respectively. Comparable results

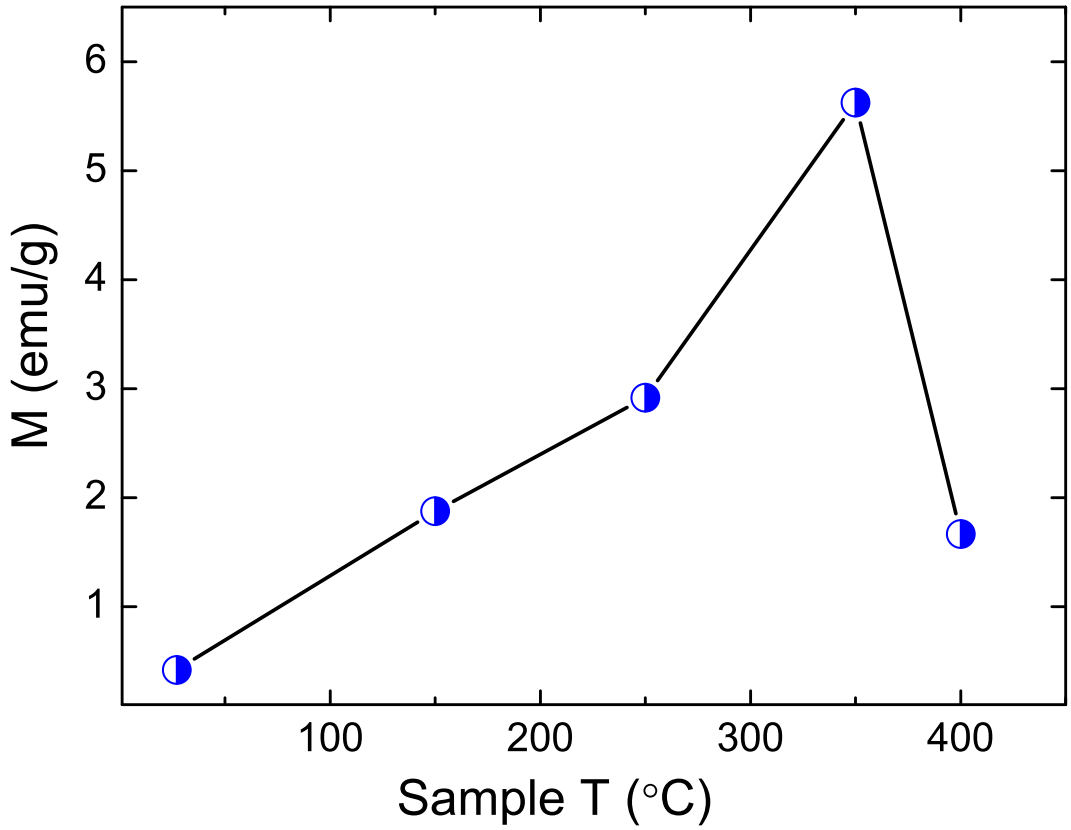

Figure 2. Room temperature saturation magnetization of the ferromagnetic signal of H-ZnO single crystals treated at different substrate temperatures, all with similar nominally implanted charge.

were reported recently [19]. The average H-concentration reached in the 20 nm surface region after 60 min implantation at the used current conditions was $\sim 2.5 \pm 0.5$ at.%. Particle induced x-ray emission (PIXE) measurements were used to analyze the magnetic impurities of the samples before and after H-treatment. There was no significant difference in the magnetic impurity concentration before and after H-plasma treatment.

Several ZnO single crystals were treated with H-plasma. All of them showed an increase in the ferromagnetic moment after H-plasma treatment relative to their virgin values. The increase of the ferromagnetic moment depends on the temperature of the sample during H-treatment at nominally similar total implanted charge. Figure 2 shows the saturation values of the ferromagnetic magnetization signal (after subtraction of the diamagnetic linear background) of several samples treated in H-plasma for 90 min at different temperatures. We found that the ferromagnetic saturation magnetization increases by increasing sample temperature and reaches a maximum at 350 °C. Therefore we concentrate on the study of samples implanted at 250 °C and 350 °C. We note that the observed dependence on the sample temperature might be very useful to control H diffusion as well as lattice defects produced during plasma treatment as well as after treatment.

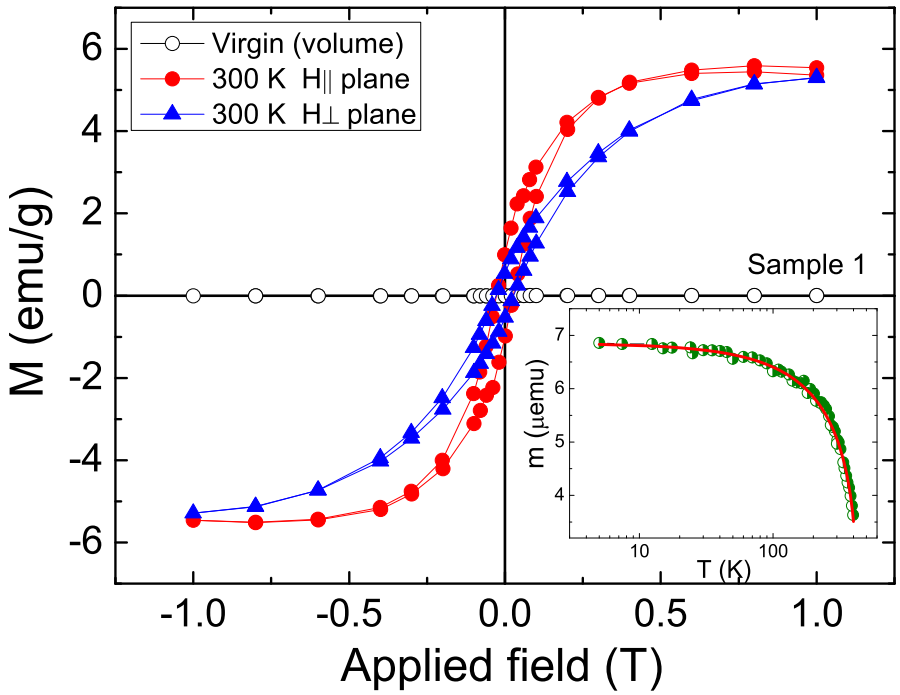

Figure 3. Hysteresis loops of a H-ZnO single crystal measured at 300 K applying a magnetic field parallel (•) and perpendicular (▲) to the main plane of the sample. The open circles (○) represent the ferromagnetic magnetization of the untreated ZnO crystal calculated by taking into account the whole volume of the sample. The diamagnetic linear background was subtracted from the measured signal. The inset shows the remanent moment vs. temperature. The (red) solid line is given by $m(T) = 6.8[\mu\text{emu}](1 - T/T_c)^{1/3})$ with a Curie temperature $T_c = 450$ K.

In what follows we discuss results of samples treated at 350 °C and 250 °C for 1 h implantation and followed by results of samples implanted at 350 °C but with different total charge (or implantation time). The results shown in this paper were not affected by aging after leaving the samples one year at 300 K.

Figure 3 shows the magnetic moment at 300 K of a H-ZnO single crystal treated at 350 °C and at applied magnetic fields parallel and perpendicular to the main sample area. Clear ferromagnetic hysteresis loops are observed at 300 K. The ferromagnetic behavior of the hysteresis shows a clear magnetocrystalline anisotropy with anisotropy constant $K_1 \sim 2 \times 10^5$ J/m^3. This anisotropy also excludes magnetic impurities as origin for the observed ferromagnetism. The remanent magnetic moment vs. temperature shown in the inset of Fig. 3 was measured at zero field after applying a field parallel to the sample main surface and cooled down in field to 5 K. The temperature dependence of the remanence follows $m(T) = m_0(1 - T/T_c)^\delta$ with $\delta = 0.33 \pm 0.05$, a static scaling law

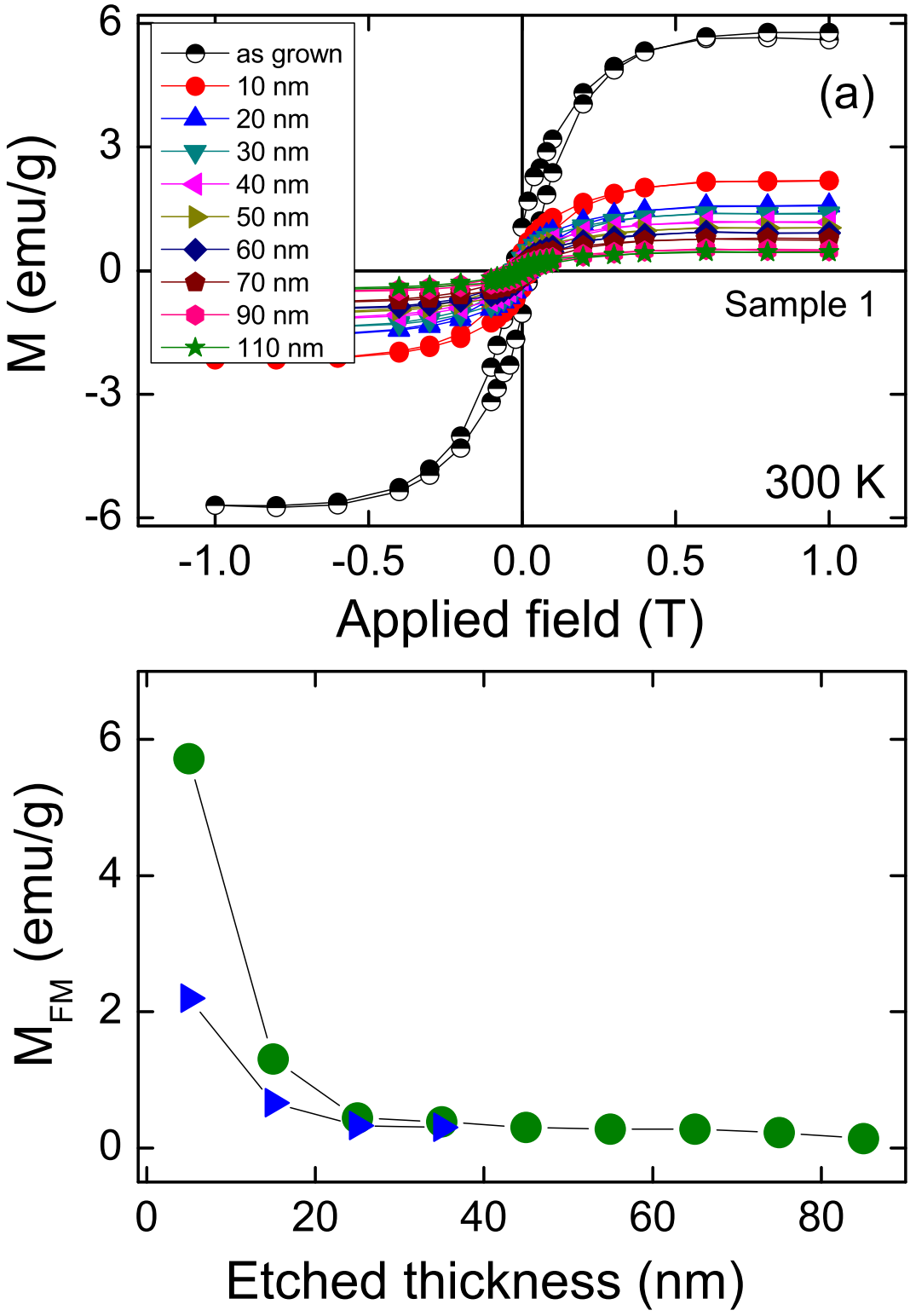

Figure 4. (a) Magnetic moment as a function of applied magnetic field of a H-ZnO single crystal at different etching stages, after subtraction of the diamagnetic contribution at 300 K. (b) Ferromagnetic magnetization values at saturation obtained taking into account the change in magnetic moment (see (a)) after etching a specific thickness of the surface region for H-treated samples at substrate temperatures of 350 °C (•) and 250 °C (▲).

with an exponent similar to other ferromagnets like e.g. $CrBr_3$[20]. This fit indicates a Curie temperature of $T_c = 450 \pm 25$ K.

In order to investigate how much surface thickness of the ZnO single crystals is contributing to the observed ferromagnetism we etched up to $\sim$ 100 nm thick layer and studied the change in ferromagnetic moment. For this purpose we used a solution of 0.3 ml HCl in 400 ml water[21, 22]. The single crystals were etched from both sides and then the measured etched mass divided by two in order to exclude the mass of H-untreated side. After $\simeq$ 40 s etching time a $\simeq$ 4 μg mass of the ZnO crystal was removed, which means $\simeq$10 nm thick layer from the H-treated side. After etching 10 nm thick layer the hysteresis loop was measured at 300 K. These results are shown in Fig. 4(a). Knowing the etched mass and the corresponding change in ferromagnetic moment we can calculate the real magnetization of the H-treated layer. The magnetization as a function of etched thickness for two samples treated at different temperatures is shown in Fig. 4(b). From these results it becomes clear that the major ferromagnetic contribution vanishes after etching the first $\simeq$20 nm layer, a layer thickness that agrees with the calculated H-concentration using SRIM and shown in Fig.1. At the used H^+-energies the estimated concentration of O- and Zn-vacancies is 8 and 9 orders of magnitude smaller than the H-concentration in the first 20 nm from the surface, see inset in Fig. 1. This huge difference clearly indicates that in the treated samples hydrogen with a concentration of several percent at the surface and not Zn- or O-vacancies or interstitials play a major role in the observed magnetic order.

We also studied the influence on the ferromagnetic signal of the amount of hydrogen implanted into the sample. The samples were treated with H-plasma at a temperature of 350 °C at 3 different total implanted times, namely 30, 60 and 90 min. The ferromagnetic signals of these samples are shown in Fig. 5. We observe that the magnetization of H-ZnO crystals increases with the total treatment time.

With the measured ferromagnetic magnetization within the first 20 nm surface region we estimate a magnetic moment of the order of 0.2 μ_B per ZnO unit cell. If we assume that in average about 1 H atom per unit cell exists in this 20 nm region then this magnetic moment triggered by each H atom is comparable to that obtained in Ref. [12].

In conclusion, we investigated the magnetic properties of remote H-plasma treated ZnO single crystals. The NRA results confirmed the enhanced concentration of hydrogen in ZnO single crystals after treatment. Characteristic ferromagnetic hysteresis loops as well as a magnetic anisotropy were observed in H-ZnO samples at room temperature. Systematically measurements of the magnetic moment of the treated samples after wet chemical etching proved that only the first $\lesssim$ 20 nm thick surface layer of H-treated ZnO contributes to the total ferromagnetic magnetization, in agreement with the expected H-penetration depth estimated by SRIM. We attribute the observed ferromagnetism in H-ZnO single crystals to the influence of hydrogen. Because hydrogen implantation also reduces dramatically the resistivity of the ZnO structure, this ferromagnetic oxide should be more easily applied in spintronic devices. Magnetotransport measurements on

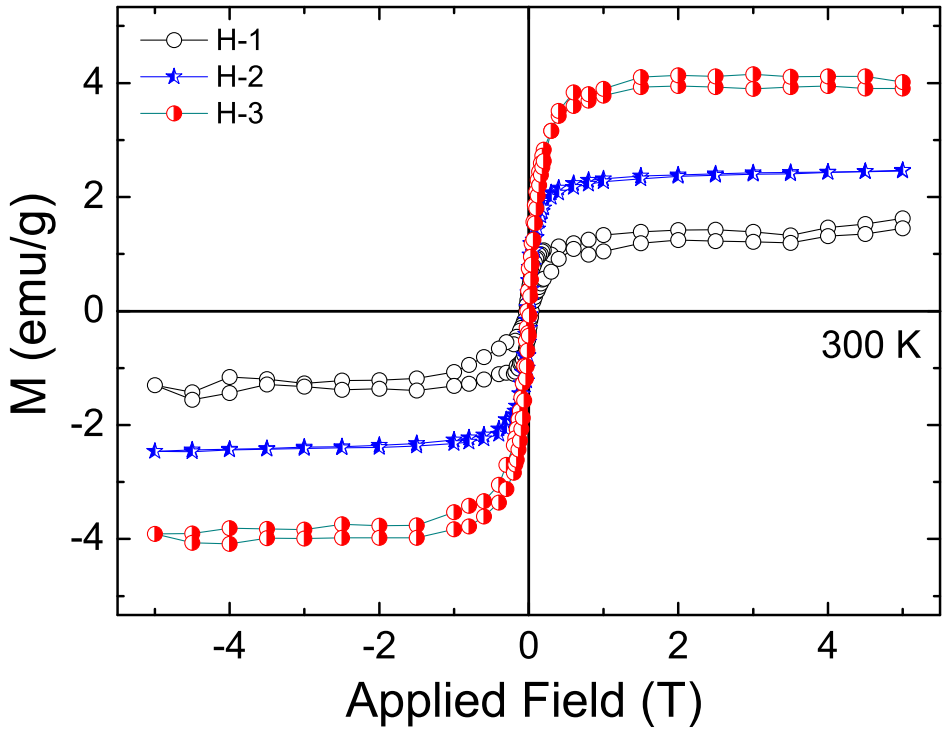

Figure 5. Magnetization of H-ZnO single crystal vs applied field measured at different total implantations. The saturation magnetization increases by increasing the implanted charge.

similar H-treated samples are currently being performed and show a negative magnetoresistance that increases (absolutely speaking) the larger the ferromagnetic magnetization (proportional to the H-concentration). Transport measurements as a function of the angle between current and applied magnetic field show a clear anisotropic magnetoresistance (AMR), which amplitude decreases as a function of temperature. At 250 K the amplitude of the AMR is $\simeq 0.5\%$ of the measured resistance at a field of 5 T. The existence of an AMR indicates a finite $L \cdot S$ coupling contribution to the scattering as well as the existence of a spin asymmetry in the electronic band. These results will be published elsewhere.

This work was supported by the DFG within the Collaborative Research Center (SFB 762) "Functionality of Oxide Interfaces".

[1] S. Banerjee, M. Mandal, N. Gayathri, and M. Sardar. Appl. Phys. Lett., 91:182501, 2007.
[2] M. Khalid, M. Ziese, A. Setzer, P. Esquinazi, M. Lorenz, H. Hochmuth, M. Grundmann, D. Spemann, T. Butz, G. Brauer, W. Anwand, G. Fischer, W. A. Adeagbo, W. Hergert, and

A. Ernst. Phys. Rev. B, 80(3):035331, Jul 2009.
[3] S. Zhou, Q. Xu, K. Potzger, G. Talut, R. Grtzschel, J. Fassbender, M. Vinnichenko, J. Grenzer, M. Helm, H. Hochmuth, M. Lorenz, M. Grundmann, and H. Schmidt. Appl. Phys. Lett., 93:232507, 2008.
[4] K.Y. Wu, Q.Q. Fang, W.N. Wang, C. Zhou, W. J. Huang, J. G. Li, Q. R. Lv, Y. M. Liu, Q.P. Zhang, and H.M. Zhang. J. of Appl. Phys., 108:063530, 2010.
[5] S. Chawla, K. Jayanthi, and R. K. Kotnala. Phys. Rev. B, 79:125204, 2009.
[6] Q. Xu, H. Schmidt, S. Zhou, K. Potzger, M. Helm, H. Hochmuth, M. Lorenz, A. Setzer, P. Esquinazi, C. Meinecke, and M. Grundmann. Appl. Phys. Lett., 92:082508, 2008.
[7] J.B. Yi, C.C. Lim, G.Z. Xing, H.M. Fan, L.H. Van, S.L. Huang, K.S. Yang, X.L. Huang, X.B. Qin, B.Y. Wang, T. Wu, L. Wang, H.T. Zhang, X.Y. Gao, T. Liu, A.T.S. Wee, Y.P. Feng, and J. Ding. Phys. Rev. Lett., 104:137201, 2010.
[8] H. Ohldag, P. Esquinazi, E. Arenholz, D. Spemann M. Rothermel, A. Setzer, and T. Butz. New J. Phys., 12:123012, 2010.
[9] C. G. Van de Walle. Phys. Rev. Lett., 85:1012, 2000.
[10] C. Wang, G. Zhou, J. Li, B. Yan, and W. Duan. Phys. Rev. B, 77:245303, 2008.
[11] C. Woll. Progress in Surf. Sci., 82:55, 2007.
[12] N. Sanchez, S. Gallego, J. Cerda, and M.C. Munoz. Phys. Rev. B, 81:115301, 2010.
[13] E.-Z. Liu, J.-F. Liu, Y. He, and J. Z. Jiang. J Magn Magn Mat, 321:3507, 2009.
[14] S. Torbrugge, F. Ostendorf, and M. Reichling. J. Phys. Chem. C, 113:4909, 2009.
[15] D.F.Wang, H.B. Lu, J.C. Li, Y. Wu, Y. Tian, and Y.P. Lee. Mat. Resch. Bulletin, 44:41, 2009.
[16] Y. M. Strzhemechny, H.L. Mosbacker, D.C. Look, D.C. Reynolds, and C.W. Litton et.al. Appl.Phys. Lett., 84:2545, 2004.
[17] W. A. Lanford. Handbook of Modern Ion Beam Materials Analysis, R. Tesmer and M. Nastasi (eds.). Materials Reseach Society, Pittsburgh, PA, 1995.
[18] J. F. Ziegler, J. P. Biersack, and U. Littmark. The stopping and range of ions in solids. Pergamon, New York, 1985.
[19] W. Anwand, G. Brauer, T. E. Cowan, D. Grambole, W. Skorupa, J. C. Čižek, J. Kuriplach, I. Procházka, W. Egger, and P. Sperr. Phys. Status Solidi A, 207:2415, 2010.
[20] John T. Ho and J. D. Litster. Phys. Rev. B, 2(11):4523–4532, Dec 1970.
[21] H. Maki, T. Ikoma, I. Sakaguchi, N. Ohashi, H. Haneda, J. Tanaka, and N. Ichinose. Thin Solid Films, 411:91, 2002.
[22] T.T. Lin and D. Lichtman. J. of Appl. Phys., 48:2164, 1977.